

5 μm , few-cycle pulses with multi-GW peak power at a 1 kHz repetition rate

LORENZ VON GRAFENSTEIN,¹ MARTIN BOCK,¹ DENNIS UEBERSCHAER,¹ KEVIN ZAWILSKI,² PETER SCHUNEMANN,² UWE GRIEBNER,^{1*} AND THOMAS ELSAESSER¹

¹Max Born Institute for Nonlinear Optics and Short Pulse Spectroscopy, Max-Born-Str. 2a, D-12489 Berlin, Germany

²BAE Systems, MER15-1813, P.O. Box 868, Nashua, New Hampshire 03061, USA

*Corresponding author: griebner@mbi-berlin.de

Received XX Month XXXX; revised XX Month, XXXX; accepted XX Month XXXX; posted XX Month XXXX (Doc. ID XXXXX); published XX Month XXXX

A mid-IR optical parametric chirped pulse amplification (OPCPA) system generating few-cycle pulses with multi-GW peak power at a 1 kHz repetition rate is reported. The system is pumped by a highly stable 2- μm picosecond chirped pulse amplifier based on Ho:YLF gain media to exploit the high nonlinearity of ZnGeP₂ (ZGP) crystals for parametric amplification. The ZGP OPA is characterized by a high conversion efficiency of >10% resulting in 1.3 mJ idler pulses at a center wavelength of 5.1 μm . Employing a dispersion management scheme only based on bulk materials pulses as short as 160 fs are obtained. Adding a spatial light modulator in the OPCPA setup the pulses are further recompressed to 75 fs duration which corresponds to less than 5 optical cycles. Taking into account the pulse energy of 0.65 mJ in this configuration it translates into a peak power of 7.7 GW. The achieved pulse durations and peak powers represent record values for high energy mid-IR OPCPAs beyond 4 μm . © 2017 Optical Society of America

OCIS codes: (140.3070) Infrared and far-infrared lasers; (140.7090) Ultrafast lasers; (190.4970) Parametric oscillators and amplifiers.

<http://dx.doi.org/10.1364/OL.99.099999>

New mid-infrared (mid-IR) laser sources providing high average output power are of tremendous scientific and technological interest [1]. The mid-IR spectral range hosts characteristic vibrational transitions of numerous molecular systems and solid materials, making mid-IR laser sources crucial for applications in spectroscopy, materials processing and chemical and biomolecular sensing. Femtosecond pulses at mid-IR wavelengths with a multi-mJ energy per pulse are a key element in strong-field physics [2] and the development of table-top sources for bright soft and hard X-ray generation [3-5]. A substantial enhancement of the femtosecond hard x-ray flux from laser-driven metal

targets has recently been demonstrated with a low-repetition rate mid-IR system [5]. In high-order harmonic generation (HHG), mJ mid-IR fs driver pulses have allowed for extending the HHG energy up to the keV range [4].

The most promising route to access the wavelength range $\lambda > 4 \mu\text{m}$ in combination with scalability of the pulse energy relies on optical parametric chirped-pulse amplification (OPCPA) [6] using non-oxide crystals like ZnGeP₂ (ZGP) or CdSiP₂ (CSP) [7]. So far, different OPCPA schemes for the mid-infrared have been explored, covering a wide range of pulse energies, durations, and repetition rates [8-13]. For most applications such sources require operation at multi-kHz repetition rates to ensure sufficient detection sensitivity and/or signal-to-noise ratio.

The pump laser is a crucial component in OPCPA because it essentially determines the performance of the whole system. Access to the relevant wavelength range above 4 μm at reasonably high parametric conversion efficiency depends critically on powerful 2- μm pump sources [7]. Pulse energies of 39 mJ at 2 μm were demonstrated by applying a cryo-cooled Ho:YLF power amplifier [14]. Pulse compression of this source yields pulses of 11 ps duration. However, this CPA operates at a fairly low repetition rate of 0.1 kHz to prevent instabilities related to the bifurcation problem [15,16]. Recently we demonstrated picosecond power amplification at 1 kHz using water-cooled Ho:YLF rods generating up to 55 mJ pulse energy [17], the highest reported for kHz CPA systems at 2 μm . Pulse compression at 25 mJ pulse energy provided almost transform-limited pulses with a duration of 4.3 ps [17].

Using few-millijoule 2- μm pump pulses with ~ 40 fs duration, pulses at wavelengths $> 4 \mu\text{m}$ have been generated via OPA at 10 Hz and 1 kHz with pulse energies of 50 μJ [9] and 30 μJ [10] and pulse durations of 450 fs [9] and 30 fs [10], respectively. Based on OPCPA with ps pump pulses at 2 μm higher pulse energies at 5 μm are generated resulting in 100 fs duration and 40 μJ energy per pulse at 1 kHz [11].

The described systems [9-11] are rather complex because each contains several OPA-stages for the 2 μm pump pulse generation. Recently, an OPCPA system delivering 180 fs pulses at 7 μm with energy of 200 μJ pumped by a rather compact 2 μm source were demonstrated. This system, however, operates at a rather low repetition rate of 100 Hz, corresponding to an average power of 55 mW with respect to the 7 μm uncompressed pulse energy [13]. A 1- μm pumped system providing mJ pulses at 3.9 μm wavelength with 20 Hz repetition rate [18] has been applied successfully to generate for soft [4] and hard X-ray pulses [5].

Here we present, to the best of our knowledge, the first millijoule-level femtosecond OPCPA source operating at kilohertz repetition rates in the mid-IR. Seeded by a compact fiber based front-end the OPCPA is pumped by a highly stable 2- μm chirped pulse amplifier (CPA) and provides pulses as short as 75 fs and pulse energies up to 1.3 mJ at a center wavelength of 5 μm .

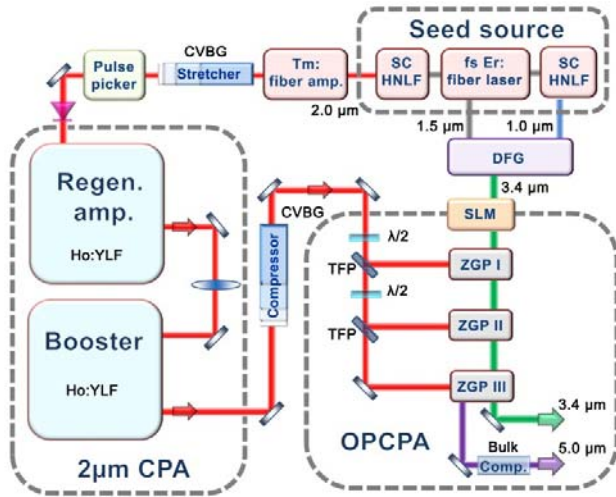


Fig. 1. Setup of the mid-IR OPCPA source pumped at 2 μm . The main parts are the seed source, the 2- μm Ho:YLF CPA amplifiers, the difference frequency generation (DFG), the spatial light modulator (SLM) and the three OPA stages based on ZGP crystals. Regen. amp., regenerative amplifier; Booster, power amplifier; CVBG, chirped volume Bragg grating; SC, supercontinuum gen.; HNLF, highly nonlinear fiber; TFP, thin-film polarize.

The layout of the 5- μm OPCPA source is presented in Fig. 1. A femtosecond Er: fiber laser operating at 40 MHz serves as master, feeding two supercontinuum (SC) sources (Toptica). This three-color front-end seeds both the OPA and the 2- μm pump channel emitting synchronized femtosecond pulses at 1.0 μm (16 mW), 1.5 μm (350 mW) and 2.0 μm (35 mW). The 2- μm pump source is similar to those reported in [16,17]. The main amplifier system is based on Ho:YLF and consists of a regenerative amplifier (RA) and two booster amplifiers, running at room temperature (Fig. 1). All amplifiers are end-pumped by randomly polarized cw Tm: fiber lasers around 1940 nm wavelength (IPG Photonics). Chirped volume Bragg gratings (CVBG, OptiGrate) are employed to stretch and compress the pulses.

The 2- μm SC output seeds the CPA pump source. The long wavelength part of the 2- μm SC spectrum is injected into a single-stage Tm: fiber pre-amplifier which is designed to amplify the spectral range from 2030 to 2110 nm (AdValue). After pre-amplification, a pulse picker reduces the 40 MHz repetition rate to 1 kHz. Subsequently, the pulses are stretched to ~ 950 ps in a CVBG designed for 2051 nm and fed into the RA. For power scaling two Ho:YLF booster amplifiers are added in a single-pass geometry, yielding up to 55 mJ pulse energy when seeding with 10 mJ RA pulses. This CPA system displays an excellent stability with a pulse-to-pulse rms as low as 0.3% [17]. This low noise level mainly originates from the Ho:YLF RA, which is optimized for stable operation in the single-energy regime. To prevent nonlinear effects and thermal problems in the available CVBGs we limited the pulse energy for compression to 25 mJ. Using one highly-dispersive CVBG (dispersion: 77 ps/nm) the pulses are moderately compressed to a duration of 30 ps. The second installed compressor scheme, a design containing two CVBGs with adapted dispersion provides shorter pulses with a duration of 4.3 ps [17].

The seed for the OPCPA is generated through difference-frequency generation (DFG) of the femtosecond pulses of the front-end, ensuring large bandwidths in the mid-IR [19]. The signal pulse is generated at 3.4 μm via DFG between the 1.0 and 1.5 μm pulses in a 1 mm long fan-out periodically poled lithium niobate crystal (MgO:PPLN). DFG yields pulses with a duration of 25 fs and a spectrum covering about 700 nm bandwidth (FWHM) (Fig. 2a).

The following spectral shaper (BNS), manufactured for the 2 to 7 μm range, is based on a 512 x 512-pixel liquid crystal (LC) spatial light modulator (SLM) with a pixel size of 37.5 μm . The SLM is implemented in a 4-f configuration using a sapphire prism as dispersive element which provides a throughput of $T=30\%$, much higher than the competing solution based on the so-called acousto-optic programmable dispersive filter (i.e. $T<10\%$).

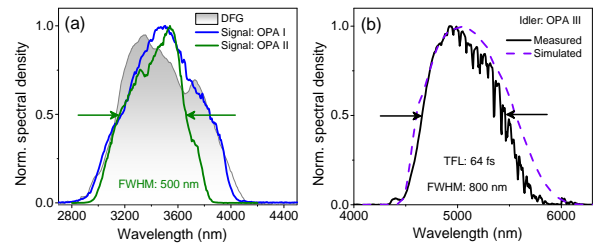


Fig. 2. Characterization of the OPCPA performance (without SLM). (a) DFG spectrum (grey), signal spectrum after the 1st (blue) and 2nd OPA stage (green), (b) idler spectrum after the 3rd OPA stage measured (black) and calculated (purple) (TFL: Fourier-transform limited).

The optical parametric amplification chain is composed of three stages, designed for different gain levels (Fig. 1). We chose ZGP crystals (BAE Systems), the most promising nonlinear material for 2- μm pumped OPCPA, which features an extremely high nonlinearity of $d_{\text{eff}}=75$ pm/V [7]. In the first two OPA stages a noncollinear geometry is applied ensuring broadband phase-matching [20]. Both contain AR-coated ZGP crystals with 5×5 mm² aperture (type-I, noncollinear angle: 2.0°, $\theta=58.6^\circ$). The optimal pump to seed

pulse duration is gain dependent [21]. Since the gain differs greatly in a multi-stage OPA, the seed pulse duration has to be adapted accordingly for each stage for optimal conversion efficiency and bandwidth. The spectral gain narrowing, which is primarily due to the high-gain first OPCA stage can be minimized by choosing a small signal-to-pump pulse duration ratio. For the subsequent low-gain stages the extraction efficiency is optimized by increasing the signal-to-pump pulse duration ratio. Taking into account the intended gain levels for the three OPA stages the signal pulses are stretched to 8 and 18 ps in front of the first and second stage, respectively, using AR-coated sapphire rods.

Seeded by the negatively chirped signal pulses and focusing the ~ 0.5 mJ pump to an intensity of 2 GW/cm^2 the first stage provided a gain $>10^5$ and spectrum as broad as the DFG without signs of gain narrowing (Fig. 2a, blue line). The 9- μJ signal pulses are then further stretched, as already described, to increase the conversion efficiency in the following OPA stages. Pumped by 2.2 mJ and similar pump intensity as in the first stage which is close to the damage threshold of ZGP, the second amplifier yields 270 μJ signal pulses. The corresponding spectrum is centered at $3.4 \mu\text{m}$ with a bandwidth of 500 nm (FWHM) indicating slight saturation as shown in Fig. 2a (green line). We are not aiming at excessive saturation to keep the Strehl ratio high for application experiments [22]. In the final stage a ZGP crystal (type-I, $\theta=56^\circ$) with a larger aperture of $10 \times 10 \text{ mm}^2$ and 2 mm thickness is employed and a collinear OPA design is chosen to prevent an angular dispersed idler. To avoid damage of the ZGP crystals only 12 mJ of the available $2 \mu\text{m}$ pulse energy is applied in the final OPA stage resulting in 1.3 mJ per pulse in the idler, the highest energy so far in the mid-IR. We achieved a noticeable energy conversion efficiency of $>10\%$ from the pump to the idler which is in good agreement with theoretical simulations of the frequency conversion process.

Given the 1 kHz repetition rate of the OPCA system a sizeable average power of 1.3 W is achieved. By blocking the signal of the OPA chain we estimate the contribution of superfluorescence to below 5%. The signal pulses at $3.4 \mu\text{m}$ with energy of 2.2 mJ are filtered out by dichroic optics. The OPCA output spectrum of the idler centered at $5.1 \mu\text{m}$ is recorded with an imaging spectrometer equipped with a cooled MCT detector and shown in Fig. 2b. The 800 nm broad (FWHM) spectrum supports a Fourier-transform limited (TFL) pulse duration of 64 fs. The small dips and the deviation with our simulation at the red edge of the spectrum are ascribed to water vapor absorption because the OPA stages are not purged.

In a first series of experiments, the compression of the positively chirped idler pulses is performed with 400 mm long CaF_2 bulk material, adjusted to compensate the introduced GDD. The compressed pulses are characterized by recording second harmonic generation frequency resolved optical gating (SHG-FROG) traces, see Fig. 3a, which yields a pulse duration of 160 fs (FWHM) corresponding to a sub-ten optical cycle signature. The retrieved pulse shape with the distinct post-pulse structure indicates a fairly large amount of uncompensated third-order dispersion (TOD) but also higher orders. During

parametric amplification, the generated idler exhibits a reversed sign of GDD relative to the signal, while the TOD does not invert the sign. Since our OPA stages are not purged the humidity in air also contributes to the TOD. Our simulation of the pulse shape (Fig. 3a, grey line) agrees well with the measurement and confirms the high amount of remaining TOD ($\sim 2 \times 10^6 \text{ fs}^3$). The latter cannot be compensated by adding further pertinent bulk material in the stretcher or compressor, because of their always positive TOD. Nonetheless, the main peak contains 66% of the pulse energy which corresponds to a sizable peak power of 5.3 GW. The nearly diffraction-limited Gaussian far-field intensity distribution and the excellent stability of the recompressed pulses at the 1 kHz repetition rate with an rms of 1.3% for a duration of one hour are presented in Fig. 3b. The results represent the first femtosecond OPCA at $\lambda > 4 \mu\text{m}$ at millijoule pulse level. Also with respect to pulse duration and stability the $5 \mu\text{m}$ OPCA outperforms competing systems [13].

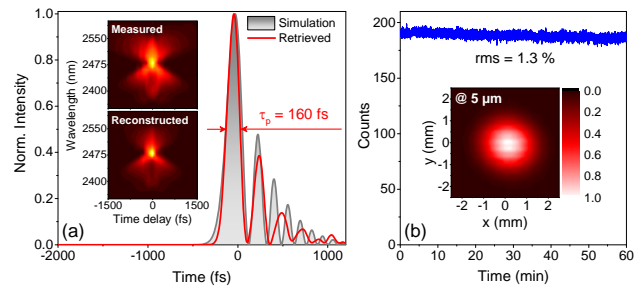


Fig. 3. Performance of the $5 \mu\text{m}$ idler pulses (OPCA without SLM). (a) SHG-FROG characterization of the compressed pulses, retrieved temporal pulse shape (red line) and simulated pulse shape (grey line), Inset: measured and retrieved SHG-FROG trace; (b) Long-term pulse stability measurement, Inset: Far-field intensity distribution.

The results in Fig. 3a show that the residual TOD is a major challenge to enter the sub-100 fs region. To compensate the residual TOD and fine-tune the GDD, the SLM is implemented in the system after the DFG for spectral phase shaping (Fig. 1). The SLM ensures more straightforward chirp compensation for the signal pulses and can also indirectly recompress the $5\text{-}\mu\text{m}$ idler pulses thanks to the chirp transfer in parametric amplification. Because of the accessible phase correction stroke of the SLM, minimization of the total TOD in the OPCA system is required. Hence the stretching/compression ratio had to be reduced by using the shorter 4.3 ps pulses of the $2\text{-}\mu\text{m}$ pump and stretching the signal pulses only after the DFG by a CaF_2 crystal to ~ 2 ps duration. The design of the three OPA stages remains unchanged except for the adaptation of the pump intensity. Now the OPCA output spectrum of the idler also extends from 4.35 to $5.50 \mu\text{m}$ at $1/e^2$, e.g., similar to the case without SLM (Fig. 2b) but with a Fourier limit of 54 fs (Fig. 4b). We attribute the more structured idler spectrum (Fig. 4b) to diffraction on the LC array of the SLM.

For bulk compression of the positively chirped idler pulses CaF_2 rods with a length of 58 mm are used. Compensating the residual GDD, TOD and fourth order dispersion of the pulses by the SLM successful recompression was achieved approaching the transform

limited duration at 650- μ J pulse energy level. The SHG-FROG trace and the retrieval results are shown in Fig. 4. The flat spectral phase confirms the excellent pulse quality (Fig. 4c, red line). The retrieved pulse shape yields a pulse duration of 75 ± 2 fs (FWHM) with an estimated energy content of 88% (Fig. 4d). The FROG-error is <1%. The recompressed pulses are not perfectly clean, but contain a small pedestal corresponding to the modulated spectrum due to diffraction on the LC array of the SLM. The main reason for the lower parametric conversion efficiency compared to the OPCPA configuration without SLM is the worse tailoring of pump and seed pulse duration.

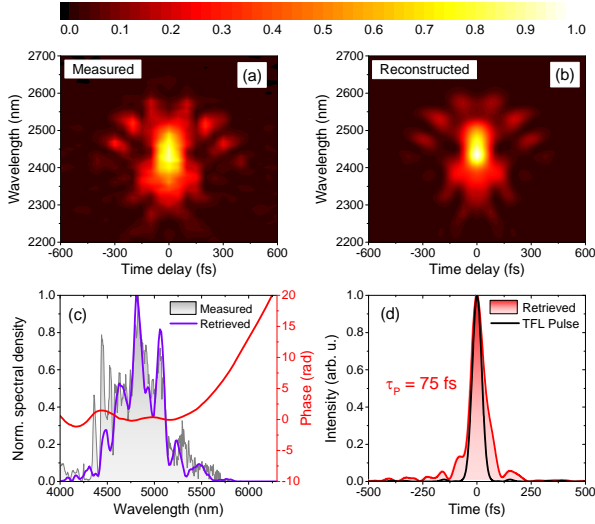


Fig. 4. SHG-FROG characterization of the 5 μ m OPCPA pulses (SLM included). (a), (b) SHG-FROG trace measured and retrieved; (c) optical spectrum, measured (grey), retrieved (purple) and phase (red); (d) retrieved temporal pulse shape (TFL: Fourier-transform limited).

The 75 fs pulse duration represents a record value for high energy mid-IR OPCPA and corresponds to only sub-five optical cycles. Taking into account the idler pulse energy of 650 μ J in this configuration, it translates into the highest peak power of 7.7 GW achieved for mid-IR OPCPAs beyond 4 μ m so far.

In conclusion, we have demonstrated a 5- μ m optical parametric chirped pulse amplification (OPCPA) system delivering multi-GW femtosecond pulses at a 1 kHz repetition rate. The system is pumped by a 2- μ m picosecond CPA based on Ho:YLF gain media to exploit the high nonlinearity of ZnGeP₂ crystals for parametric amplification. In the 1 kHz pulse train, up to 1.3 mJ idler pulses were generated and compressed to 160 fs duration by dispersion management based only on bulk materials. The pulse energy represents the highest to date of any femtosecond mid-IR source beyond 4 μ m. The OPCPA is characterized by an excellent stability with a pulse-to-pulse rms as low as 1.3%. Adding a spatial light modulator in the setup pulse compression at 0.65 mJ pulse energy was performed. The resulting pulse duration of 75 fs corresponds to a sub-five-cycle signature and is close to the Fourier-limit. This pulse characteristics represents the highest peak power of 7.7 GW achieved for 5- μ m OPCPA systems to the best of our

knowledge, and, if focused to a 15- μ m spot diameter, would reach a peak intensity of $\sim 9 \times 10^{15}$ W/cm². The system appears scalable with respect to repetition rate via a pulse picking rate in the 1 to 10 kHz range and with respect to the mid-IR pulse energy by using ZGP or CSP crystals with a larger aperture for parametric amplification driven with the full available 2- μ m pump energy of 50 mJ.

Funding. This work has been funded through the SAW grant no. SAW-2014-MBI-1 of the Leibniz Gemeinschaft and has been partly supported from the EU Laserlab programme, grant no. 654148.

Acknowledgment. We thank Gunnar Arisholm from the Norwegian Defence Research Establishment for useful discussions.

References

1. I. T. Sorokina and K. L. Vodopyanov (eds.), *"Solid-State Mid-Infrared laser sources"*, Springer (2003).
2. B. Wolter, M. G. Pullen, M. Baudisch, M. Sclafani, M. Hemmer, A. Senftleben, C. D. Schröter, J. Ullrich, R. Moshhammer, and J. Biegert, *Phys. Rev. X* **5**, 021034 (2015).
3. K.-H. Hong, C.-J. Lai, J. P. Siqueira, P. Kroger, J. Moses, C.-L. Chang, G. J. Stein, L. E. Zapata, and F. X. Kärtner, *Opt. Lett.* **39**, 3145 (2014).
4. T. Popmintchev, M.-C. Chen, D. Popmintchev, P. Arpin, S. Brown, S. Ališauskas, G. Andriukaitis, T. Balčiūnas, O. D. Mücke, A. Pugžlys, A. Baltuška, B. Shim, S. E. Schrauth, A. Gaeta, C. Hernández-García, L. Plaja, A. Becker, A. Jaron-Becker, M. M. Murnane, and H. C. Kapteyn, *Science* **336**, 1287 (2012).
5. J. Weissaupt, V. Juvé, M. Holtz, S. A. Ku, M. Woerner, T. Elsaesser, S. Ališauskas, A. Pugžlys, and A. Baltuška, *Nat. Photonics* **8**, 927 (2014).
6. J. Rothhardt, S. Hädrich, J. C. Delagnes, E. Cormier, and J. Limpert, *Las. Photon. Rev.* **11**, 170043 (2017).
7. V. Petrov, *Progress in Quantum Electron.* **42**, 1 (2015).
8. J. Biegert, P. K. Bates, and O. Chalus, *IEEE J. Sel. Top. Quantum Electron.* **18**, 531 (2012).
9. S. Wandel, G. Xu, Y. Yin, and I. Jovanovic, *J. Phys. B: At. Mol. Opt. Phys.* **47**, 234016 (2014).
10. P. Kroger, H. Liang, K. Zawilski, P. Schunemann, T. Lang, U. Morgner, J. Moses, F. X. Kärtner, and K.-H. Hong, *CLEO2016*, paper Stu3I.4.
11. T. Kanai, P. Malevich, S. S. Kangaparambil, K. Ishida, M. Mizui, K. Yamanouchi, H. Hoogland, R. Holzwarth, A. Pugžlys, and A. Baltuška, *Opt. Lett.* **42**, 683 (2017).
12. M. Mero and V. Petrov, *IEEE Photon. Journal* **93**, 200408 (2017).
13. D. Sanchez, M. Hemmer, M. Baudisch, S. L. Cousin, K. Zawilski, P. Schunemann, O. Chalus, C. Simon-Boisson, and J. Biegert, *Optica* **3**, 147 (2016).
14. M. Hemmer, D. Sánchez, M. Jelínek, Vadim Smirnov, H. Jelinkova, V. Kubeček, and J. Biegert, *Opt. Lett.* **40**, 451 (2015).
15. M. Grishin, V. Gulbinas, and A. Michailovas, *Opt. Express* **15**, 9434 (2007).
16. L. von Grafenstein, M. Bock, G. Steinmeyer, U. Griebner, and T. Elsaesser, *Las. Photon. Rev.* **10**, 123 (2016).
17. L. von Grafenstein, M. Bock, D. Ueberschaer, U. Griebner, and T. Elsaesser, *Opt. Lett.* **41**, 4668 (2016).
18. G. Andriukaitis, T. Balčiūnas, S. Ališauskas, A. Pugžlys, A. Baltuška, T. Popmintchev, M.-C. Chen, M. M. Murnane, and H. C. Kapteyn, *Opt. Lett.* **36**, 2755 (2011).
19. C. Erny, K. Moutzouris, J. Biegert, D. Kuhlke, F. Adler, A. Leitenstorfer, and U. Keller, *Opt. Lett.* **32**, 1138 (2007).
20. T. Lang, T. Binhammer, S. Rausch, G. Palmer, M. Emons, M. Schultze, A. Harth, and U. Morgner, *Opt. Express* **20**, 912 (2012).
21. J. Moses, C. Manzoni, S.-W. Huang, G. Cerullo, and F. X. Kärtner, *Opt. Express* **17**, 5540 (2009).
22. A. Giree, M. Mero, G. Arisholm, M. J. J. Vrakking, and F. J. Furch, *Opt. Express* **25**, 3104 (2017).

References

1. I. T. Sorokina and K. L. Vodopyanov (eds.), *"Solid-State Mid-Infrared laser sources"*, Springer (2003).
2. B. Wolter, M. G. Pullen, M. Baudisch, M. Sclafani, M. Hemmer, A. Senftleben, C. D. Schröter, J. Ullrich, R. Moshhammer, and J. Biegert, "Strong-Field Physics with Mid-IR Fields," *Phys. Rev. X* **5**, 021034 (2015).
3. K.-H. Hong, C.-J. Lai, J. P. Siqueira, P. Kroger, J. Moses, C.-L. Chang, G. J. Stein, L. E. Zapata, and F. X. Kärtner, "Multi-mJ, kHz, 2.1 μm optical parametric chirped-pulse amplifier and high-flux soft x-ray high-harmonic generation," *Opt. Lett.* **39**, 3145–3148 (2014).
4. T. Popmintchev, M.-C. Chen, D. Popmintchev, P. Arpin, S. Brown, S. Ališauskas, G. Andriukaitis, T. Balčiūnas, O. D. Mücke, A. Pugžlys, A. Baltuška, B. Shim, S. E. Schrauth, A. Gaeta, C. Hernández-García, L. Plaja, A. Becker, A. Jaron-Becker, M. M. Murnane, and H. C. Kapteyn, "Bright coherent ultrahigh harmonics in the keV X-ray regime from mid-infrared femtosecond lasers," *Science* **336**, 1287 (2012).
5. J. Weisshaupt, V. Juvé, M. Holtz, S. A. Ku, M. Woerner, T. Elsaesser, S. Ališauskas, A. Pugžlys, and A. Baltuška, "High-brightness table-top hard x-ray source driven by sub-100 femtosecond mid-infrared pulses," *Nat. Photonics* **8**, 927–930 (2014).
6. J. Rothhardt, S. Hädrich, J. C. Delagnes, E. Cormier, and J. Limpert, "High average power near-infrared few-cycle lasers," *Las. Photon. Rev.* **11**, 170043 (2017).
7. V. Petrov, "Frequency down-conversion of solid-state laser sources to the mid-infrared spectral range using non-oxide nonlinear crystals," *Progress in Quantum Electron.* **42**, 1 (2015).
8. J. Biegert, P. K. Bates, and O. Chalus, "New mid-infrared light sources," *IEEE J. Sel. Top. Quantum Electron.* **18**, 531 (2012).
9. S. Wandel, G. Xu, Y. Yin, and I. Jovanovic, "Parametric generation of energetic short mid-infrared pulses for dielectric laser acceleration," *J. Phys. B: At. Mol. Opt. Phys.* **47**, 234016 (2014).
10. P. Kroger, H. Liang, K. Zawilski, P. Schunemann, T. Lang, U. Morgner, J. Moses, F. X. Kärtner, and K.-H. Hong, "Octave spanning 1.5-optical-cycle 6.5- μm OPA pumped by 2.1- μm OPCPA," *CLEO2016*, paper St31.4.
11. T. Kanai, P. Malevich, S. S. Kangaparambil, K. Ishida, M. Mizui, K. Yamanouchi, H. Hoogland, R. Holzwarth, A. Pugžlys, and A. Baltuška, "Parametric amplification of 100 fs mid-infrared pulses in ZnGeP_2 driven by a Ho:YAG chirped pulse amplifier," *Opt. Lett.* **42**, 683 (2017).
12. M. Mero and V. Petrov, "High-power, few-cycle angular dispersion compensated mid-infrared pulses from a noncollinear optical parametric amplifier," *IEEE Photon. Journal* **93**, 200408 (2017).
13. D. Sanchez, M. Hemmer, M. Baudisch, S. L. Cousin, K. Zawilski, P. Schunemann, O. Chalus, C. Simon-Boisson, and J. Biegert, "7 μm , ultrafast, sub-millijoule-level mid-infrared optical parametric chirped pulse amplifier pumped at 2 μm ," *Optica* **3**, 147 (2016).
14. M. Hemmer, D. Sánchez, M. Jelínek, Vadim Smirnov, H. Jelinkova, V. Kubeček, and J. Biegert, "2- μm wavelength, high-energy Ho:YLF chirped-pulse amplifier for mid-infrared OPCPA," *Opt. Lett.* **40**, 451–454 (2015).
15. M. Grishin, V. Gulbinas, and A. Michailovas, "Dynamics of high repetition rate regenerative amplifiers," *Opt. Express* **15**, 9434–9443 (2007).
16. L. von Grafenstein, M. Bock, G. Steinmeyer, U. Griebner, and T. Elsaesser, "Taming chaos: 16 mJ picosecond Ho:YLF regenerative amplifier with 0.7 kHz repetition rate," *Las. Photon. Rev.* **10**, 123–130 (2016).
17. L. von Grafenstein, M. Bock, D. Ueberschaer, U. Griebner, and T. Elsaesser, "Ho:YLF chirped pulse amplification at kilohertz repetition rates - 4.3 ps pulses at 2 μm with GW peak power," *Opt. Lett.* **41**, 4668–4671 (2016).
18. G. Andriukaitis, T. Balčiūnas, S. Ališauskas, A. Pugžlys, A. Baltuška, T. Popmintchev, M.-C. Chen, M. M. Murnane, and H. C. Kapteyn, "90 GW peak power few-cycle mid-infrared pulses from an optical parametric amplifier," *Opt. Lett.* **36**, 2755 (2011).
19. C. Erny, K. Moutzouris, J. Biegert, D. Kühlke, F. Adler, A. Leitenstorfer, and U. Keller, "Mid-infrared difference-frequency generation of ultrashort pulses tunable between 3.2 and 4.8 μm from a compact fiber source," *Opt. Lett.* **32**, 1138–1140 (2007).
20. T. Lang, T. Binhammer, S. Rausch, G. Palmer, M. Emons, M. Schultze, A. Harth, and U. Morgner, "High power ultra-widely tuneable femtosecond pulses from a non-collinear optical parametric oscillator (NOPO)," *Opt. Express* **20**, 912–917 (2012).
21. J. Moses, C. Manzoni, S.-W. Huang, G. Cerullo, and F. X. Kärtner, "Temporal optimization of ultrabroadband high-energy OPCPA," *Opt. Express* **17**, 5540–5555 (2009).
22. A. Giree, M. Mero, G. Arisholm, M. J. J. Vrakking, and F. J. Furch, "Numerical study of spatiotemporal distortions in noncollinear optical parametric chirped-pulse amplifiers," *Opt. Express* **25**, 3104–3121 (2017).

Title:

5 μm few-cycle pulses with multi-gigawatt peak power at a 1 kHz repetition rate

Authors:

L. von Granfenstein, M. Bock, D. Ueberschaer, K. Zawilski, P. Schunemann, U. Griebner, and T. Elsaesser

Manuscript

The original publication may be found at:

Journal: Optics Letters, Vol. 42, No. 19 / 2017 / 3796-3799

DOI: <https://doi.org/10.1364/OL.42.003796>